DALTON

Electrochemical oxidation and protonation of a bridging amide ligand at a dinuclear metal–sulfur site †

François Y. Pétillon, Philippe Schollhammer and Jean Talarmin *

UMR 6521 Chimie, Electrochimie Moléculaires et Chimie Analytique, Université de Bretagne Occidentale, 6 Av. V Le Gorgeu, BP 809, 29285 Brest Cedex, France

The electrochemical oxidation of the amide complex $[Mo_2(cp)_2(\mu\text{-}SMe)_3(\mu\text{-}NH_2)]$ **1** (cp = η^5-C_5H_5) has been investigated in tetrahydrofuran (thf) and MeCN electrolytes by cyclic voltammetry, controlled-potential electrolysis and coulometry. The two-electron oxidation of **1** leads to the release of a proton and to the formation of the imide derivative $[Mo_2(cp)_2(\mu\text{-}SMe)_3(\mu\text{-}NH)]^+$ **2**. In MeCN, this reaction is reversible. The protonation of **1** has been shown to produce a complex in which a NH_3 ligand is bound to a Mo centre; the protonated complex is stabilized by co-ordination of the anion of the acid, of the solvent or of a substrate to the neighbouring metal centre. The protonation performed in thf in the presence of chloride produces $[Mo_2(cp)_2(\mu\text{-}SMe)_3(\mu\text{-}Cl)]$ which is the precursor of the amide complex **1**. The final protonation product formed in MeCN is $[Mo_2(cp)_2(\mu\text{-}SMe)_3(MeCN)_2]^+$, which also is a precursor of **1**. Therefore, these experiments allow the construction of a hydrazine disproportionation cycle.

The chemistry of transition-metal complexes with sulfide, thiolate or thioether ligands has been widely investigated since these compounds are seen as models for the species involved in biological processes or in catalytic reactions of industrial importance.[1–8] In the past few years, our studies of dinuclear, thiolate-bridged complexes have focused on site–substrate interactions and recognition phenomena. In this context, we have investigated the electrochemical generation $\{M_2(\mu\text{-}SR)_n\}$ sites (M = Mo, W or V) and their reactivity towards unsaturated substrates (cyanide, nitriles or isocyanides), with the objective of understanding the factors which control the reactivity of metal complexes towards substrates, as well as the origins of their selectivity.[9] The control of electronic and steric parameters of the co-ordination sphere could eventually allow the design of versatile substrate-binding sites, or on the contrary, the construction of selective sites containing the information which could be recognized by a given substrate, such as dinitrogen. However, although we have improved the stability of complexes with weakly bonded substrates (acetonitrile) by modifying the electron density at the metal centres,[9c] we have not been able yet to synthesize dinitrogen derivatives with a $\{M_2(\mu\text{-}SR)_n\}$ core. Therefore, in order to introduce a {N–N} fragment in our complexes, which would permit the study of the transformations of nitrogenous ligands co-ordinated to two metal–sulfur centres, we treated $[Mo_2(cp)_2(\mu\text{-}SMe)_3(\mu\text{-}Cl)]$ (cp = η^5-C_5H_5) with hydrazine; this resulted in the quantitative formation of $[Mo_2(cp)_2(\mu\text{-}SMe)_3(\mu\text{-}NH_2)]$.[10] Metalloamide complexes are interesting in the context of nitrogen fixation since they are thought to be involved as intermediates in the biological reduction of N_2 to ammonia.[11] The special interest of $[Mo_2(cp)_2(\mu\text{-}SMe)_3(\mu\text{-}NH_2)]$ in this context lies in the fact that the amide ligand is co-ordinated to a $Mo_2(SR)_3$ centre. The present paper describes the oxidative electrochemistry and the protonation of $[Mo_2(cp)_2(\mu\text{-}SMe)_3(\mu\text{-}NH_2)]$.

Results and Discussion

Electrochemical oxidation of $[Mo_2(cp)_2(\mu\text{-}SMe)_3(\mu\text{-}NH_2)]$ 1

Cyclic voltammetry (CV) of the amide complex $[Mo_2(cp)_2(\mu\text{-}SMe)_3(\mu\text{-}NH_2)]$ **1** has been investigated in tetrahydrofuran (thf) and MeCN electrolytes; pertinent redox potentials are listed in Table 1. The CV of **1** in these electrolytes presents some common features, but also a few differences are noted. For example, the first oxidation of **1** is a quasi-reversible, diffusion-controlled one-electron step in both solvents $[(i_p^c/i_p^a)_{ox1} \approx 1$ for 0.02 V $s^{-1} \leqslant \nu \leqslant 1$ V s^{-1}; $i_p^{a}{}_{ox1}/\nu^{1/2}$ independent of scan rate, $\Delta E_p > 60$ mV] ‡ (Figs. 1 and 2). Three oxidation peaks, as well as the irreversible reduction of the complex ($E_{p\,red} = -3.4$ V) are observed in thf–$[NBu_4][PF_6]$, whereas the CV in MeCN–$[NBu_4][PF_6]$ shows four oxidation systems; the reduction of **1** takes place at a potential which is too negative for detection in MeCN. The reversibility of the second oxidation step is different in thf and in MeCN and this process is described below.

thf–$[NBu_4][PF_6]$ Electrolyte. The second oxidation of **1** is irreversible, even at low temperature and for scan rates $\nu \leqslant 1$ V s^{-1}, which indicates that chemical reaction(s) is (are) coupled after the electron-transfer (EC) process.[12] The product generated at the second oxidation by the EC process oxidizes quasi-reversibly at $E^{1/2} = 0.53$ V and undergoes an irreversible reduction at −1.22 V. Another minor, quasi-reversible couple is also present on the reverse scan after the second oxidation of **1** has been traversed (Fig. 1). The potential of this couple ($E^{1/2} = -0.45$ V) is close to that measured for the species resulting from the protonation of **1** by aqueous HBF_4 (see below), which suggests that the chemical step following the second oxidation of **1** might consist in the release of a proton.

Controlled-potential electrolysis (CPE) performed at the potential of the first oxidation of **1** leads to high yields (*ca.* 80%§) of the corresponding radical cation after consumption of 0.95 ± 0.05 F mol^{-1} **1** [Fig. 3(*b*)]. Electrolyses conducted at the potential of the radical cation oxidation are completed after the passage of a further 0.8–0.9 F mol^{-1} starting material and lead to the product detected by CV before electrolysis [Fig. 3(*c*)]. The nature of this complex, *i.e.* the imide derivative $[Mo_2(cp)_2$-

† Based on the presentation given at Dalton Discussion No. 2, 2nd–5th September 1997, University of East Anglia, UK.

‡ The parameters i_p^a and i_p^c are respectively the anodic and the cathodic peak currents of a reversible redox process, ΔE_p is the separation between these peaks; for a reversible one-electron system ΔE_p is close to 60 mV. For the reversible oxidation of ferrocene we find ΔE_p of 70 mV (MeCN) and *ca.* 90–100 mV (thf); ν is the scan rate; an EC process comprises an electron-transfer step (E) followed by a chemical reaction (C).

§ The yields were estimated by CV, from the comparison of the peak current of the reactant complex to that of the product of the reaction (controlled-potential electrolysis or protonation), assuming identical diffusion coefficients.

Table 1 Redox potentials of the complexes

Complex	Solvent	$E^{1/2}_{ox1}$/V *vs.* $Fe(cp)_2$–$Fe(cp)_2^+$	$E^{1/2}_{ox2}$/V *vs.* $Fe(cp)_2$–$Fe(cp)_2^+$	$E_{p\,red}$/V *vs.* $Fe(cp)_2$–$Fe(cp)_2^+$
1 $[Mo_2(cp)_2(\mu\text{-}SMe)_3(\mu\text{-}NH_2)]$	thf	−0.64	0.07 (irrev)[a]	−3.39
	MeCN	−0.65	0.09[b]	—
2 $[Mo_2(cp)_2(\mu\text{-}SMe)_3(\mu\text{-}NH)]^+$	thf	0.56 (irrev) 0.52 (0.5 V s^{-1})	—	−1.26[c]
	MeCN	0.57 0.50 (−46 °C)	—	−1.17[d]
$[Mo_2(cp)_2(\mu\text{-}SMe)_3(NH_3)(TsO)]$	thf	−0.60	0.05	−2.50
$[Mo_2(cp)_2(\mu\text{-}SMe)_3(NH_3)(CF_3CO_2)]$	thf	−0.57	0.08	−2.76
$[Mo_2(cp)_2(\mu\text{-}SMe)_3(NH_3)(thf)]^+$	thf	−0.39	0.31	−2.35
$[Mo_2(cp)_2(\mu\text{-}SMe)_3(NH_3)(CNBu^t)]^+$	thf	−0.33	0.46 (irrev) 0.63 (irrev)	−2.26
$[Mo_2(cp)_2(\mu\text{-}SMe)_3(NH_3)(CNxyl)]^+$	thf	−0.29	0.65 (irrev)	−2.05
$[Mo_2(cp)_2(\mu\text{-}SMe)_3(NH_3)(MeCN)]^+$	MeCN	−0.35	0.39	−2.26

[a] Product peaks are observed at $E^{1/2}_{ox} = 0.53$ and $E_{p\,red} = -1.22$ V. [b] Product peaks are observed at $E_{p\,ox} = 0.58$ and $E_{p\,red} = -1.12$ V. [c] Product peaks are observed at $E^{1/2}_{ox} = -0.66$ and $E_{p\,red} = -2.51$ V. [d] Product peaks are observed at $E^{1/2}_{ox} = -0.65$ and $E_{p\,red}$ *ca.* −2.4 V.

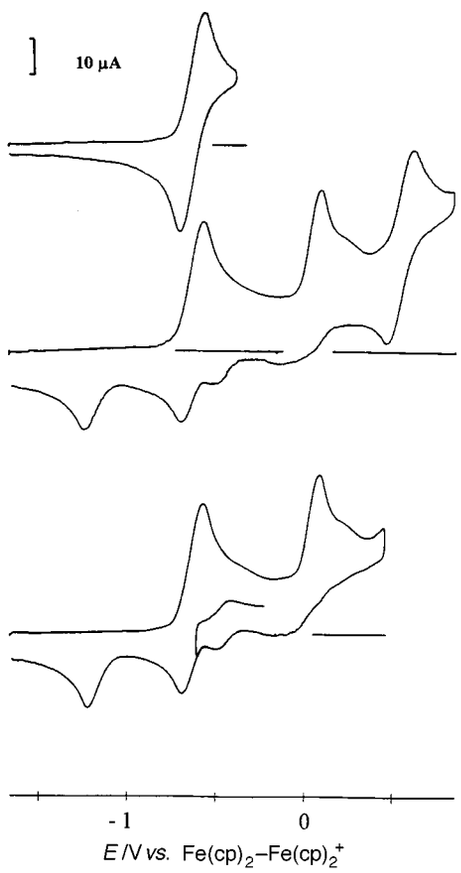

Fig. 1 Cyclic voltammetry of $[Mo_2(cp)_2(\mu\text{-}SMe)_3(\mu\text{-}NH_2)]$ **1** (*ca.* 2 mM) in thf–$[NBu_4][PF_6]$ (vitreous carbon electrode, scan rate: 0.2 V s^{-1})

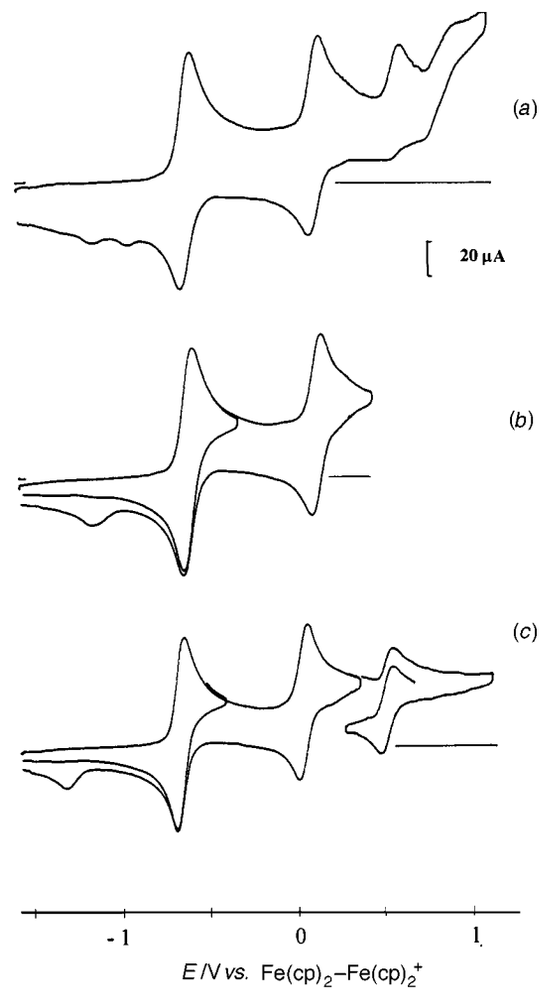

Fig. 2 Cyclic voltammetry of $[Mo_2(cp)_2(\mu\text{-}SMe)_3(\mu\text{-}NH_2)]$ **1** (2.2 mM) in MeCN–$[NBu_4][PF_6]$ at room temperature (*a*,*b*) and at −46 °C (*c*) (vitreous carbon electrode, scan rate: 0.2 V s^{-1})

$(\mu\text{-}SMe)_3(\mu\text{-}NH)]^+$ **2** has been confirmed by ^1H NMR spectroscopy of the product extracted from the anolyte after controlled-potential oxidation in thf–$Li(ClO_4)$, and by comparison with the redox and spectroscopic data of an authentic sample of $[Mo_2(cp)_2(\mu\text{-}SMe)_3(\mu\text{-}NH)]^+$ obtained by a different route[13] (Table 2).

MeCN–$[NBu_4][PF_6]$ Electrolyte. The metal product resulting from the oxidation of **1** in this solvent is also **2**, as evidenced by a comparison with the redox potentials of an authentic sample of the imide complex. The mechanism of its formation is detailed now. Variable scan rate CV ($0.02 \leqslant \nu \leqslant 1$ V s^{-1}) in a potential range including the first three oxidation peaks shows that (*i*) the peak current of the second oxidation, which is a quasi-reversible process [Fig. 2(*b*)], is less than that of the first; the peak current ratio ($0.75 \leqslant i_{p\,ox2}/i_{p\,ox1} \leqslant 0.85$) is independent of ν, (*ii*) the peak current ratio $i_{p\,ox3}/i_{p\,ox1}$ decreases with increasing scan rate, (*iii*) the third oxidation shows reversibility for scan rate $\nu \geqslant 0.4$ V s^{-1} or at low temperature, under which conditions the last oxidation step is absent [Fig. 2(*c*)]. These observations indicate that the second anodic step is due to the oxidation of $\mathbf{1}^{\bullet+}$ whereas the third oxidation arises from the imide complex generated at $E_{p\,ox1}$ or $E_{p\,ox2}$. The CV on the first two oxidation systems shows that the second oxidation remains quasi-reversible at slow scan rates with $(i_p^c/i_p^a)_{ox2} \approx 0.8$–0.9 for $\nu = 0.02$ V s^{-1}. This is diagnostic of a reversible chemical reaction following a reversible charge transfer (EC_{rev}[12]). Lowering

Table 2 The ^{1}H NMR data of the complexes $[Mo_2(cp)_2(\mu\text{-}SMe)_3(NH)]BF_4$, $[Mo_2(cp)_2(\mu\text{-}SMe)_3(NH_3)(TsO)]$, $[Mo_2(cp)_2(\mu\text{-}SMe)_3(NH_3)(CNR)]BF_4$ (R = Bu^t or xyl)

Complex	δ(^{1}H)
$[Mo_2(cp)_2(\mu\text{-}SMe)_3(NH)]BF_4$ [a,b]	20.43 (s, 1 H, NH), 6.38 (s, 10 H, C_5H_5), 2.19 (s, 3 H, SCH_3), 1.79 (s, 3 H, SCH_3), 1.55 (s, 3 H, SCH_3)
$[Mo_2(cp)_2(\mu\text{-}SMe)_3(NH_3)(TsO)]$ [c]	7.7–7.1 (m, 5 H, $CH_3C_6H_4SO_3$), 6.76 (s, 5 H, C_5H_5), 5.52 (s, 5 H, C_5H_5), 2.75 (s, 3 H, NH_3), 2.33 (s, 3 H, $CH_3C_6H_4SO_3$), 2.26 (s, 3 H, SCH_3), 2.24 (s, 3 H, SCH_3), 1.24 (s, 3 H, SCH_3)
$[Mo_2(cp)_2(\mu\text{-}SMe)_3(NH_3)(CNxyl)]BF_4$ [d]	7.15–6.76 [m, 3 H, $C_6H_3(CH_3)_2NC$], 5.40 (s, 5 H, C_5H_5), 5.26 (s, 5 H, C_5H_5), 2.34 [s, 6 H, $C_6H_3(CH_3)_2NC$], 2.16 (s, 3 H, NH_3), 2.00 (s, 3 H, SCH_3), 1.80 (s, 3 H, SCH_3), 1.48 (s, 3 H, SCH_3)
$[Mo_2(cp)_2(\mu\text{-}SMe)_3(NH_3)(CNBu^t)]BF_4$ [d] (two products)	Major isomer (65%): 5.25 (s, 5 H, C_5H_5), 5.20 (s, 5 H, C_5H_5), 2.05 (s, 3 H, NH_3), 1.88 (s, 3 H, SCH_3), 1.73 (s, 3 H, SCH_3), 1.42 [s, 9 H, $C(CH_3)_3$], 1.32 (s, 3 H, SCH_3) Minor isomer (35%): 5.30 (s, 5 H, C_5H_5), 5.26 (s, 5 H, C_5H_5), 1.99 (s, 3 H, NH_3), 1.44 [s, 9 H, $C(CH_3)_3$], 1.41 (s, 3 H, SCH_3), 1.38 (s, 3 H, SCH_3), 1.36 (s, 3 H, SCH_3)

[a] In $CDCl_3$. [b] $[Mo_2(cp)_2(\mu\text{-}SMe)_3(NH)]BF_4$: IR (KBr cm^{-1}): 3270m ν(NH), 1150–950s ν(BF). [c] In CD_2Cl_2. [d] In $CDCl_3$.

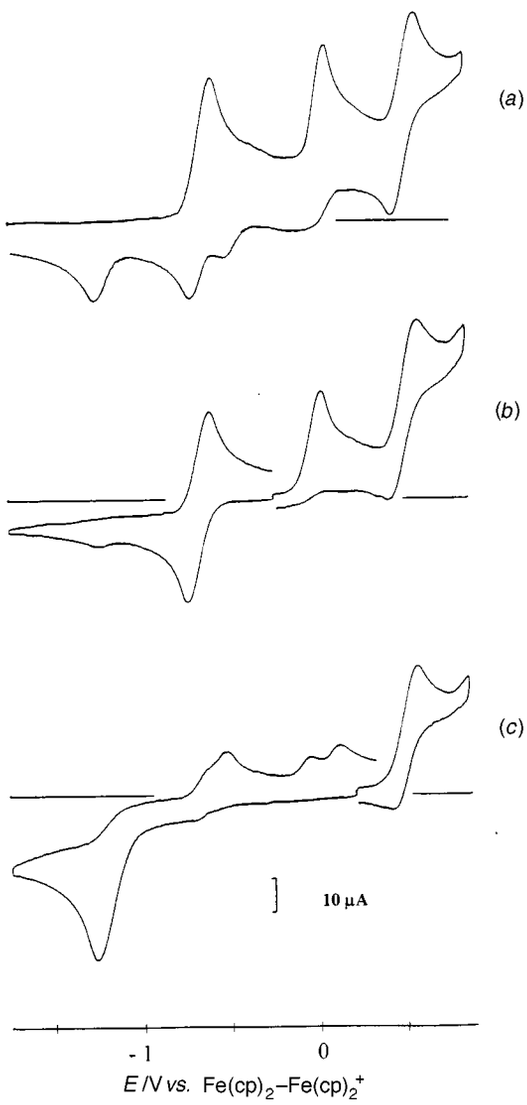

Fig. 3 Cyclic voltammetry of $[Mo_2(cp)_2(\mu\text{-}SMe)_3(\mu\text{-}NH_2)]$ (1.6 mM) in thf–$[NBu_4][PF_6]$ before (*a*) and after (*b*) controlled-potential oxidation at −0.24 V (Pt anode; 0.95 F mol^{-1} **1**); (*c*) solution in (*b*) after controlled-potential oxidation at 0.22 V (Pt anode, 0.85 F mol^{-1} **1**) (vitreous carbon electrode, scan rate: 0.2 V s^{-1})

the temperature causes a slowing down of the rate of the forward chemical reaction since the third anodic peak is substantially suppressed [Fig. 2(*c*)]. The imide derivative resulting from the chemical reaction is characterized by an irreversible reduction ($E_{p\,red} = -1.12$ V), and by an oxidation which is reversible at low temperature ($E^{1/2}{}_{ox} = 0.50$ V) [Fig. 2(*c*)]. The more anodic process is due to the product of the irreversible oxidation of the imide complex at room temperature, and will not be discussed.

The CV of the anolyte obtained after successive electrolyses of **1** at the potential of the first (0.9 F mol^{-1} **1**, average yield ≥90%§) and of the second (*ca.* 0.8 F mol^{-1} **1**) oxidation in MeCN–$[NBu_4][PF_6]$ shows three reduction steps (Fig. 4). The first broad, quasi-reversible peak ($E_{p\,red1}$) is due to the $\mathbf{1}^{2+}$–$\mathbf{1}^{\bullet+}$ couple. The second reduction is irreversible and is slightly shifted in the positive direction with respect to the $E^{1/2}$ of the reversible $\mathbf{1}^{\bullet+}$–**1** couple. Scan reversal at a potential negative of $E_{p\,red2}$ shows the presence of a reversible process with $E^{1/2} = -0.35$ V [Fig. 4(*a*)], which is fully consistent with the release of a proton on two-electron oxidation of **1**. Indeed, the stepwise addition of 1 equivalent toluene-*p*-sulfonic acid (HTsO) to $\mathbf{1}^{\bullet+}$ electrogenerated in MeCN–$[NBu_4][PF_6]$ leads to loss of reversibility of the $\mathbf{1}^{\bullet+}$–**1** couple and to a positive shift of the corresponding peak. Furthermore, a reversible system assigned to the oxidation of the protonated complex, $[Mo_2(cp)_2(\mu\text{-}SMe)_3(NH_3)(MeCN)]^+$ (see below), is observed under these conditions at $E^{1/2} = -0.35$ V. Finally, variable scan rate CV in a potential range including the three reduction peaks in Fig. 4 shows that the current ratio of the third to the first reduction peaks ($i_{p\,red3}/i_{p\,red1}$) increases with increasing scan rate, which confirms the presence of an equilibrium involving $\mathbf{1}^{2+}$ and the imide complex, reducible at $E_{p\,red3} = -1.12$ V. This suggests that controlled potential reduction of the imide complex in the presence of protons could lead to the amide derivative [Fig. 4(*b*)]. This possibility is currently investigated. These results are consistent with the reactions shown in Scheme 1, steps A–C, with the chemical step C being reversible in MeCN. Oxidation of an amide ligand to the corresponding imide has already been reported for mononuclear molybdenum and tungsten complexes.[14]

Protonation of $[Mo_2(cp)_2(\mu\text{-}SMe)_3(\mu\text{-}NH_2)]$ 1

Complex **1** reacts readily with acids; monitoring by cyclic voltammetry of the stepwise addition of HX ($X^- = TsO^-$ or $CF_3CO_2^-$) to a thf–$[NBu_4][PF_6]$ solution of **1** shows that, after 1 equivalent of acid has been added, the starting material has been totally replaced by a new species showing two quasi-reversible oxidation steps (Fig. 5, Table 1). The addition of a second equivalent of HX does not lead to further change of the CV. The presence of isopotential points[15] on the voltammograms (Fig. 5, $X^- = TsO^-$) demonstrates that the reaction is quantitative, while the dependence of the redox potentials on the nature of the acid (Table 1, $X^- = TsO^-$ or $CF_3CO_2^-$) indicates that the protonated complex contains X^-. This is consistent with proton attack at the amide ligand resulting in bridge opening, and stabilization of the NH_3 complex by coordination of X^- (Scheme 2). This is confirmed by ^{1}H NMR spectroscopy of the protonated complex ($X^- = TsO^-$, Table 2).

As shown in Scheme 2, the anion of the acid is important in

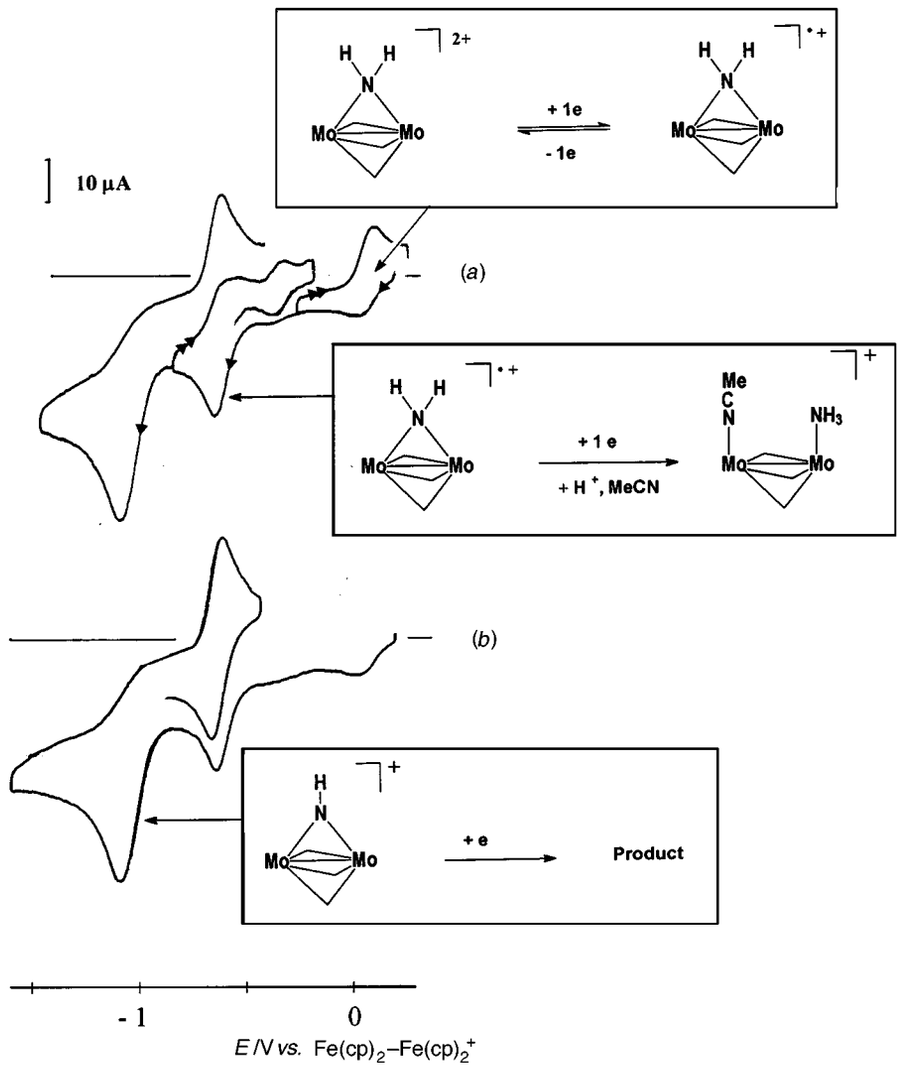

Fig. 4 Cyclic voltammetry of $[Mo_2(cp)_2(\mu\text{-}SMe)_3(\mu\text{-}NH_2)]$ **1** (1.8 mM) in MeCN–$[NBu_4][PF_6]$ after controlled-potential oxidation at −0.1 (0.96 F mol^{-1} **1**) and 0.3 V (*ca.* 0.8 F mol^{-1} **1**) (vitreous carbon electrode, scan rate: 0.2 V s^{-1})

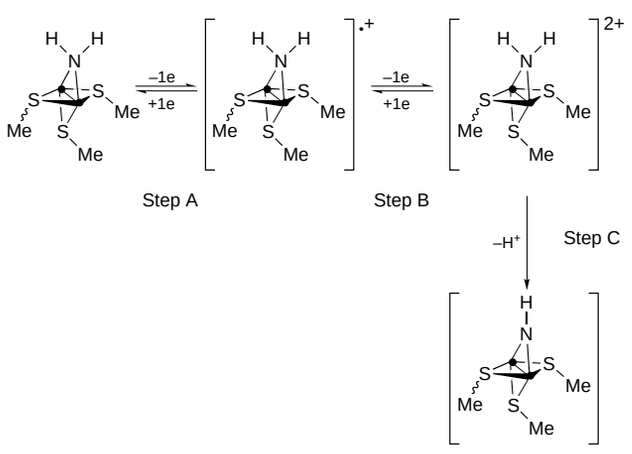

Scheme 1 ● = Mo(cp). Step C is reversible in MeCN–$[NBu_4][PF_6]$

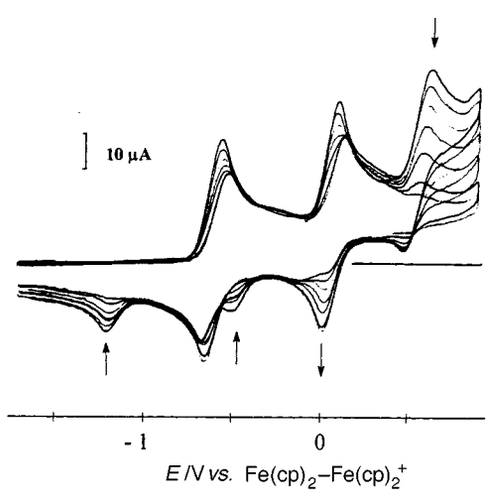

Fig. 5 Cyclic voltammetric monitoring of the stepwise addition of 1 equivalent HTsO to $[Mo_2(cp)_2(\mu\text{-}SMe)_3(\mu\text{-}NH_2)]$ **1** (1.5 mM) in thf–$[NBu_4][PF_6]$ (vitreous carbon electrode, scan rate: 0.2 V s^{-1})

stabilizing the protonated complex. Protonation of **1** by an acid with a non-co-ordinating anion (HBF_4) has also been investigated in thf–$[NBu_4][PF_6]$. The major product of the reaction of **1** with $HBF_4{\cdot}Et_2O$, characterized by quasi-reversible oxidation steps at −0.39 and 0.31 V, could not be isolated as it underwent transformation during work-up; it is tentatively assigned as $[Mo_2(cp)_2(\mu\text{-}SMe)_3(NH_3)(thf)]^+$. When $[Mo_2(cp)_2(\mu\text{-}SMe)_3(\mu\text{-}NH_2)]$ is treated with HBF_4 in the presence of TsO^- (1 equivalent), $[Mo_2(cp)_2(\mu\text{-}SMe)_3(NH_3)(TsO)]$ is observed, while $[Mo_2(cp)_2(\mu\text{-}SMe)_3(NH_3)(CNR)]^+$ [R = Bu^t or xyl (xyl = 2,6-$Me_2C_6H_3$)] is formed when the protonation is conducted in the presence of 1 equivalent RNC (Tables 1 and 2). The latter is also obtained on addition of excess RNC to $[Mo_2(cp)_2(\mu\text{-}SMe)_3(NH_3)(TsO)]$. The linear plot (Fig. 6) of $E^{1/2}_{ox1}$ of the protonated complexes against the ligand constant P_L [16] (L = $CF_3CO_2^-$, P_L = −0.78;[16] Bu^tNC, −0.44;[17] thf, −0.57;[18] for L = xylNC, we used the same P_L value as for PhNC, −0.38 [16]) is consistent

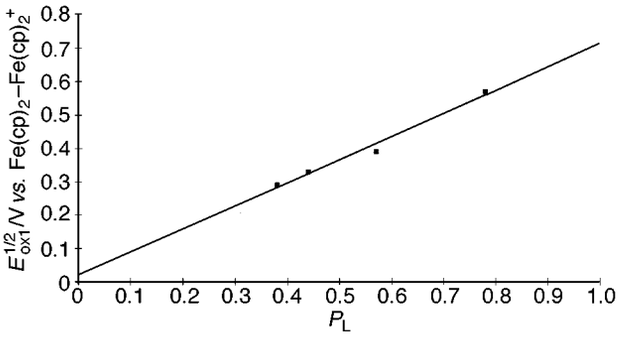

Fig. 6 Plot of $E^{1/2}_{ox1}$ of the protonated complexes $[Mo_2(cp)_2(\mu\text{-}SMe)_3(NH_3)(L \text{ or } X^-)]^+$ *vs.* the ligand constant P_L[16] (L or X^- = xylNC, Bu^tNC, thf or $CF_3CO_2^-$)

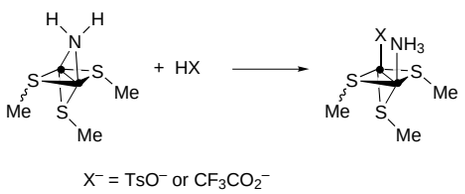

Scheme 2 ● = Mo(cp)

with the formation of a thf derivative when the protonation is effected in the absence of any co-ordinating anion or substrate.

However, the reaction of **1** with $HBF_4 \cdot Et_2O$ is less clean than that with HTsO or CF_3CO_2H, and unidentified species are also formed. Protonation with aqueous HBF_4 also gives rise to several products, characterized by a broad, quasi-reversible oxidation around −0.45 V and overlapping processes with $E^{1/2}_{ox}$ at −0.04 and 0.09 V. These results suggest that in the case of acids with non-co-ordinating anions, the protonation in thf–$[NBu_4][PF_6]$ leads to $[Mo_2(cp)_2(\mu\text{-}SMe)_3(NH_3)(L)]^+$ complexes where L = thf and/or H_2O. The reaction of $[Mo_2(cp)_2(\mu\text{-}SMe)_3(\mu\text{-}NH_2)]$ with HCl is different from the previous ones in that 2 equivalents of acid are needed for the reaction to reach completion. The metal-containing product formed quantitatively§ under these conditions is $[Mo_2(cp)_2(\mu\text{-}SMe)_3(\mu\text{-}Cl)]$, while the only complexes observed by cyclic voltammetric monitoring of the stepwise addition of HCl in thf–$[NBu_4][PF_6]$ are the starting material and the μ-Cl complex.¶ The stoichiometry of the reaction and the nature of the final product indicate that the protonated species $[Mo_2(cp)_2(\mu\text{-}SMe)_3(NH_3)(X)]$ (Scheme 3, step A) is not indefinitely stable for $X^- = Cl^-$; the substitution of the NH_3 ligand by a chloride lone pair would lead to the observed product (Scheme 3, step B) and the release of ammonia. That $[Mo_2(cp)_2(\mu\text{-}SMe)_3(Cl)(NH_3)]$ is not detected by CV suggests that this step is faster than step A. Finally, the protonation of NH_3 (Scheme 3, step C) released before the starting material had been completely consumed accounts for the observed stoichiometry. Such a role of the chloride ligand has already been observed. The irreversible reduction (EC process) of the stable radical cation $[Mo_2(cp)_2(\mu\text{-}SMe)_3(Cl)(MeCN)]^{\cdot+}$ produces $[Mo_2(cp)_2(\mu\text{-}SMe)_3(\mu\text{-}Cl)]$, *via* the short-lived, undetected $[Mo_2(cp)_2(\mu\text{-}SMe)_3(Cl)(MeCN)]$ intermediate, and the subsequent fast substitution of the remaining MeCN ligand by the chloride lone pair.[9b] Furthermore, the reaction of $[Mo_2(cp)_2(\mu\text{-}SMe)_3(MeCN)_2]^+$ with Cl^- also leads to $[Mo_2(cp)_2(\mu\text{-}SMe)_3(\mu\text{-}Cl)]$, presumably *via* the same intermediate.[9b] Thus, the particularity of the protonation by HCl lies in the fact that the anion of this acid can assume a bridging position and favours the release of ammonia. This has been confirmed in the following way: treatment of $[Mo_2(cp)_2(\mu\text{-}SMe)_3(\mu\text{-}NH_2)]$ with aqueous HBF_4 in the presence of chloride (NEt_4Cl, 1.5 equivalents) in thf–$[NBu_4][PF_6]$ also requires the addition of 2 equivalents acid and produces the μ-chloride compound; furthermore, the release of ammonia induced by Cl^- binding is evidenced by the formation of $[Mo_2(cp)_2(\mu\text{-}SMe)_3(\mu\text{-}Cl)]$ on addition of chloride to $[Mo_2(cp)_2(\mu\text{-}SMe)_3(NH_3)(TsO)]$.

¶ Isopotential points are observed.

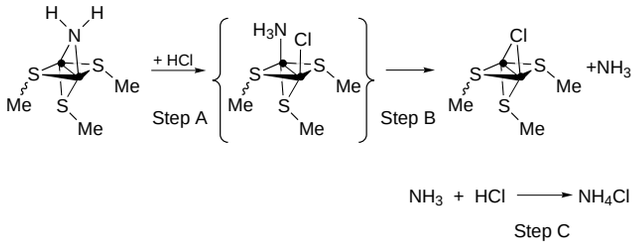

Scheme 3 ● = Mo(cp)

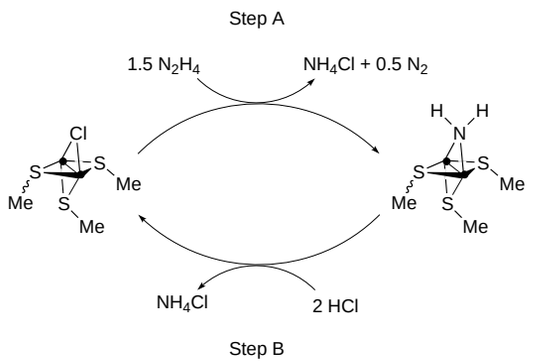

Scheme 4 ● = Mo(cp)

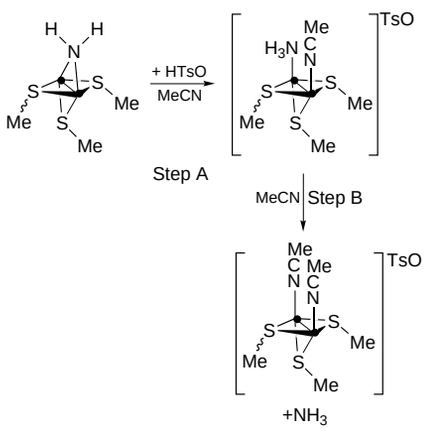

Scheme 5 ● = Mo(cp)

The ultimate intermediate of the reduction of N_2 to NH_3 at a metal centre is likely to be an amino complex, and the question is how is ammonia released in the last step of the reduction cycle.[14] In this context, the deco-ordination of ammonia assisted by the chloride ligand as described above is interesting to note; we have already emphasized the similarity between the function of the chloride bridge in our complexes and that of an organic hemilabile ligand.[9b] The above results show that protonation of the amide complex by HCl, or by HX in the presence of chloride, allows a hydrazine disproportionation cycle to be completed (Scheme 4, step B).

Protonation of $[Mo_2(cp)_2(\mu\text{-}SMe)_3(\mu\text{-}NH_2)]$ by HTsO or aqueous HBF_4 (1 equivalent) in MeCN eventually produces $[Mo_2(cp)_2(\mu\text{-}SMe)_3(MeCN)_2]^+$ *via* an intermediate whose conversion to the final product can be monitored by CV. The intermediate was assigned as $[Mo_2(cp)_2(\mu\text{-}SMe)_3(NH_3)(NCMe)]^+$ since its redox potentials (Table 1) are similar to those of $[Mo_2(cp)_2(\mu\text{-}SMe)_3(NH_3)(CNR)]^+$ (Scheme 5). Since $[Mo_2(cp)_2(\mu\text{-}SMe)_3(\mu\text{-}NH_2)]$ can be prepared by treating $[Mo_2(cp)_2(\mu\text{-}SMe)_3(MeCN)_2]^+$ with hydrazine,[19] the protonation of the amide complex in MeCN (Scheme 5) provides another means of completing a hydrazine disproportionation cycle. The reaction in Scheme 5 shows some similarity with the

protonation of **1** by HCl in thf, in that the NH_3 ligand is released. However, the different stoichiometry indicates that the slow step in Scheme 3 is not the same as in Scheme 5. Indeed, the CV detection of $[Mo_2(cp)_2(\mu\text{-}SMe)_3(NH_3)(MeCN)]^+$ (Scheme 5) demonstrates that in this case, step A is faster than step B whereas it is the opposite in Scheme 3. The protonation of **1** by HCl (2 equivalents) in MeCN leads to a mixture of the μ-chloride complex and of the bis(MeCN) cation. This is consistent with the occurrence of an equilibrium between these compounds, which can be shifted towards $[Mo_2(cp)_2(\mu\text{-}SMe)_3(\mu\text{-}Cl)]$ or $[Mo_2(cp)_2(\mu\text{-}SMe)_3(MeCN)_2]^+$ by addition of chloride or H^+, respectively.[9b]

Conclusion

The results reported in this paper illustrate the reactivity of an amide ligand bridging two metal centres in a sulfur environment. (1) The electrochemical 2e oxidation of $[Mo_2(cp)_2(\mu\text{-}SMe)_3(\mu\text{-}NH_2)]$ produces the corresponding imide complex. In MeCN in the presence of H^+, the latter is in equilibrium with $[Mo_2(cp)_2(\mu\text{-}SMe)_3(\mu\text{-}NH_2)]^{2+}$: this indicates the possibility of reducing $[Mo_2(cp)_2(\mu\text{-}SMe)_3(\mu\text{-}NH)]^+$ to the amide in the presence of protons. (2) Proton attack at the amide bridge in $[Mo_2(cp)_2(\mu\text{-}SMe)_3(\mu\text{-}NH_2)]$ produces a species containing an NH_3 ligand co-ordinated to a $Mo(SMe)_3$ centre, while the anion of the acid ($X^- = TsO^-$, $CF_3CO_2^-$ or Cl^-) or a solvent molecule binds to the neighbouring metal atom in order to stabilize the protonated complex. Importantly, this step leads to the release of ammonia when $X^- = Cl^-$. These results demonstrate that an amide ligand, which is believed to be an intermediate in the biological nitrogen fixation process, can be protonated to ammonia at a dinuclear sulfur-co-ordinated metal site. Further studies concerning the reduction of the imide complex $[Mo_2(cp)_2(\mu\text{-}SMe)_3(\mu\text{-}NH)]^+$ are currently in progress in our group.

Experimental

Methods and materials

All the experiments were carried out under an inert atmosphere, using Schlenk techniques for the syntheses. Tetrahydrofuran (thf) was purified as described previously.[20] Acetonitrile (Carlo Erba or BDH, HPLC grade) was used as received. The acids, toluene-*p*-sulfonic (Prolabo), trifluoroacetic (Aldrich), fluoroboric (diethyl ether complex and aqueous solution, Aldrich), were used as received. The preparation and the purification of the supporting electrolyte $[NBu_4][PF_6]$ and the electrochemical equipment were as described previously.[20] All the potentials are quoted against the ferrocene–ferrocenium couple; ferrocene was added as an internal standard at the end of the experiments. Proton NMR spectra were recorded on a Bruker AC300 spectrometer. Shifts are relative to tetramethylsilane as an internal reference. Chemical analyses were performed by the Centre de Microanalyses du CNRS, Vernaison. The complexes $[Mo_2(cp)_2(\mu\text{-}SMe)_3(\mu\text{-}NH_2)]$[10] and $[Mo_2(cp)_2(\mu\text{-}SMe)_3(MeCN)_2]^+$[9b] were synthesized according to literature methods.

Syntheses

$[Mo_2(cp)_2(\mu\text{-}SMe)_3(NH_3)(TsO)]$. To a solution of $[Mo_2(cp)_2(\mu\text{-}SMe)_3(\mu\text{-}NH_2)]$ (0.20 g, 0.4 mmol) in thf (5 cm^3) was added 1 equivalent of HTsO. The solution turned instantly from orange to green. Addition of diethyl ether (10 cm^3) precipitated $[Mo_2(cp)_2(\mu\text{-}SMe)_3(NH_3)(TsO)]$ as a brownish green solid (yield: 0.23 g, 90%).

$[Mo_2(cp)_2(\mu\text{-}SMe)_3(NH_3)(thf)]BF_4$. To a solution of $[Mo_2(cp)_2(\mu\text{-}SMe)_3(\mu\text{-}NH_2)]$ (0.20 g, 0.4 mmol) in thf (5 cm^3) was added 1 equivalent of $HBF_4{\cdot}Et_2O$. The solution turned instantly from orange to green. Addition of diethyl ether (10 cm^3) precipitated $[Mo_2(cp)_2(\mu\text{-}SMe)_3(NH_3)(thf)]^+$ as a green solid but fast decomposition occurred when the thf was filtered off.

$[Mo_2(cp)_2(\mu\text{-}SMe)_3(NH_3)(CNR)]BF_4$ (R = Bu^tNC or xylNC). To a solution of $[Mo_2(cp)_2(\mu\text{-}SMe)_3(\mu\text{-}NH_2)]$ (0.20 g, 0.4 mmol) and of isocyanide (1 equivalent, R = Bu^t or xyl) in thf (5 cm^3) was added 1 equivalent of $HBF_4{\cdot}Et_2O$. Addition of diethyl ether (10 cm^3) precipitated $[Mo_2(cp)_2(\mu\text{-}SMe)_3(NH_3)(CNR)]BF_4$ as a brown solid, *ca.* 90% yield (R = $C_6H_3Me_2$, 0.25 g; Bu^t, 0.23 g). R = $C_6H_3Me_2$ (Found: C, 36.9; H, 4.4; N, 3.9. Calc. for $C_{24}H_{31}BF_4Mo_2N_2S_3$: C, 37.8; H, 4.5; N, 4.0%). IR (KBr pellet)/cm^{-1}: 3390w, 3330w, 3280vw ν(NH), 2040s, 1980 (sh) ν(CN) and 1150–950s ν(BF). R = Bu^t. IR (KBr pellet)/cm^{-1}: 3400w, 3350w, 3290w, ν(NH), 2100s, 2040sh ν(CN) and 1150–1000s ν(BF).

Acknowledgements

The CNRS (Centre National de la Recherche Scientifique) and UBO (Université de Bretagne Occidentale) are acknowledged for financial support.

References

1 R. H. Holm and E. D. Simhon, in *Metal Ions in Biology*, ed. T. G. Spiro, Wiley, New York, 1985, vol. 7, ch. 1, p. 1; R. H. Holm, *Adv. Inorg. Chem*., 1992, **38**, 1.
2 D. Coucouvanis, *ACS Symp. Ser*., 1993, **535**, 304.
3 D. Sellmann, *ACS Symp. Ser*., 1993, **535**, 332.
4 M. Hidai and Y. Mizobe, *Chem. Rev*., 1995, **95**, 1115.
5 B. C. Gates, J. R. Katzer and G. C. A. Shuit, *Chemistry of Catalytic Processes*, McGraw-Hill, New York, 1979.
6 M. Rakowski DuBois, *Chem. Rev*., 1989, **89**, 1; P. Bernatis, J. C. V. Laurie and M. Rakowski DuBois, *Organometallics*, 1990, **9**, 1607; C. J. Casewit, D. E. Coons, L. L. Wright, W. K. Miller and M. Rakowski DuBois, *Organometallics*, 1986, **5**, 951; M. Rakowski DuBois, M. C. Vanderveer, D. L. DuBois, R. C. Haltiwanger and W. K. Miller, *J. Am. Chem. Soc*., 1980, **102**, 7456.
7 B. C. Wiegand and C. M. Friend, *Chem. Rev*., 1992, **92**, 491.
8 U. Riaz, O. J. Curnow and M. D. Curtis, *J. Am. Chem. Soc*., 1991, **113**, 1416; U. Riaz, O. J. Curnow and M. D. Curtis, *J. Am. Chem. Soc*., 1994, **116**, 4357.
9 (*a*) F. Gloaguen, C. Le Floch, F. Y. Pétillon, J. Talarmin, M. El Khalifa and J. Y. Saillard, *Organometallics*, 1991, **10**, 2004; (*b*) F. Barrière, Y. Le Mest, F. Y. Pétillon, S. Poder-Guillou, P. Schollhammer and J. Talarmin, *J. Chem. Soc*., *Dalton Trans*., 1996, 3967; (*c*) F. Y. Pétillon, S. Poder-Guillou, P. Schollhammer and J. Talarmin, *New J. Chem*., 1997, **21**, 477; (*d*) M. L. Abasq, D. L. Hughes, F. Y. Pétillon, R. Pichon, C. J. Pickett and J. Talarmin, *J. Chem. Soc*., *Dalton Trans*., 1997, 2279.
10 P. Schollhammer, F. Y. Pétillon, S. Poder-Guillou, J. Y. Saillard, J. Talarmin and K. W. Muir, *Chem. Commun*., 1996, 2633.
11 M. Y. Mohammed and C. J. Pickett, *J. Chem. Soc*., *Chem. Commun*., 1988, 1119; D. L. Hughes, D. J. Lowe, M. Y. Mohammed, C. J. MacDonald and C. J. Pickett, *Polyhedron*, 1989, **8**, 1653; C. J. Pickett, *J. Bioinorg. Chem*., 1996, **1**, 601.
12 A. J. Bard and L. R. Faulkner, in *Electrochemical Methods. Fundamentals and Applications*, Wiley, New York, 1980, ch. 11, pp. 429–485; E. R. Brown and R. F. Large, in *Techniques of Chemistry*, ed. A. Weissberger, Wiley, New York, 1971, vol. I, ch. 6, pp. 423–530.
13 K. W. Muir, P. Schollhammer, F. Y. Pétillon and J. Talarmin, unpublished work.
14 T. E. Glassman, M. G. Vale and R. R. Schrock, *Organometallics*, 1991, **10**, 4046.
15 J. G. Gaudiello, T. C. Wright, R. A. Jones and A. J. Bard, *J. Am. Chem. Soc*., 1985, **107**, 888; A. Fitch and G. J. Edens, *J. Electroanal. Chem*., *Interfacial Electrochem*., 1989, **267**, 1.
16 J. Chatt, C. T. Kan, G. J. Leigh, C. J. Pickett and D. R. Stanley, *J. Chem. Soc*., *Dalton Trans*., 1980, 2032.
17 A. J. L. Pombeiro, C. J. Pickett and R. L. Richards, *J. Organomet. Chem*., 1982, **224**, 285.
18 T. I. Al Salih and C. J. Pickett, *J. Chem. Soc*., *Dalton Trans*., 1985, 1255.
19 P. Schollhammer, F. Y. Pétillon and J. Talarmin, unpublished work.
20 M. L. Abasq, F. Y. Pétillon, P. Schollhammer and J. Talarmin, *New J. Chem*., 1996, **20**, 1221.

Received 6*th June* 1997; *Paper* 7/03959J